The Effects of Inhibition of MicroRNA-375 in a Mouse Model of Doxorubicin-Induced Cardiac Toxicity

Authors' Contribution:
Study Design A
Data Collection B
Statistical Analysis C
Data Interpretation D
Manuscript Preparation E
Literature Search F
Funds Collection G

ABCDE Hao Zhang
ABCE Yikui Tian
BCD Degang Liang
BCDE Qiang Fu
BCD Liqun Jia
BC Dawei Wu
ABCDEF Xinyuan Zhu

Department of Cardiovascular Surgery, Tianjin Medical University General Hospital, Tianjin, P.R. China

Corresponding Author: Xinyuan Zhu, e-mail: zxytmu@163.com
Source of support: Departmental sources

Background: Doxorubicin-induced myocardial toxicity is associated with oxidative stress, cardiomyocyte, apoptosis, and loss of contractile function. Previous studies showed that microRNA-375 (miR-375) expression was increased in mouse models of heart failure and clinically, and that inhibition of miR-375 reduced inflammation and increased survival of cardiomyocytes. This study aimed to investigate the effects and mechanisms of inhibition of miR-375 in a mouse model of doxorubicin-induced cardiac toxicity *in vivo* and in doxorubicin-treated rat and mouse cardiomyocytes *in vitro*.

Material/Methods: The mouse model of doxorubicin-induced cardiac toxicity was developed using an intraperitoneal injection of doxorubicin (15 mg/kg diluted in 0.9% saline) for eight days. Treatment was followed by a single subcutaneous injection of miR-375 inhibitor. H9c2 rat cardiac myocytes and adult murine cardiomyocytes (AMCs) were cultured *in vitro* and treated with doxorubicin, with and without pretreatment with miR-375 inhibitor.

Results: Doxorubicin significantly upregulated miR-375 expression *in vitro* and *in vivo*, and inhibition of miR-375 re-established myocardial redox homeostasis, prevented doxorubicin-induced oxidative stress and cardiomyocyte apoptosis, and activated the PDK1/AKT axis by reducing the direct binding of miR-375 to 3' UTR of the PDK1 gene. Inhibition of PDK1 and AKT abolished the protective role of miR-375 inhibition on doxorubicin-induced oxidative damage.

Conclusions: Inhibition of miR-375 prevented oxidative damage in a mouse model of doxorubicin-induced cardiac toxicity *in vivo* and in doxorubicin-treated rat and mouse cardiomyocytes *in vitro* through the PDK1/AKT signaling pathway.

MeSH Keywords: Apoptosis • Doxorubicin • Oxidative Stress

Full-text PDF: https://www.medscimonit.com/abstract/index/idArt/920557

📄 4002　📊 —　📈 7　📚 39

Background

Doxorubicin is a broad-spectrum and highly effective chemotherapeutic agent that has been used in the treatment of human malignant neoplasms [1]. However, its clinical use is commonly associated with several side effects, including irreversible myocardial toxicity that gradually progresses to congestive heart failure [2]. No optimal therapeutic approaches are currently available to prevent doxorubicin-induced myocardial toxicity or to protect the myocardium due to the complex pathophysiological mechanisms involved.

Previous studies have shown that doxorubicin can accumulate within the myocardium and is retained within the inner membrane of mitochondria by forming a stable complex with cardiolipin [3]. These effects destroy the normal mitochondrial ultrastructure and function, leading to an unrestrained generation of reactive oxygen species (ROS) [3]. Doxorubicin also has a strong affinity for iron, and the formation of doxorubicin and iron complexes triggers the accumulation of oxidants through a Fenton-type reaction in which hydrogen peroxide is catalyzed to highly toxic hydroxyl free radicals [4]. Also, the quinine moiety in doxorubicin can be reduced to an intermediate molecule by flavoprotein reductases, and the reduced form of doxorubicin promotes the generation of superoxide anions in the presence of molecular oxygen [5,6]. Chaiswing et al. found that reactive oxygen species (ROS) could be detected in heart tissue within three hours after doxorubicin injection [7]. Increased ROS generation results in oxidative damage to biological macromolecules and provokes extrinsic and intrinsic apoptotic signaling. Therefore, oxidative stress is an important initiating factor and is involved in the progression of doxorubicin-induced cardiomyocyte death and cardiac dysfunction. It is possible that approaches to reduce ROS overexpression may prevent or treat doxorubicin-induced myocardial toxicity.

MicroRNAs (miRNAs) have recently been identified and are a class of evolutionarily conserved, single-stranded molecules that negatively regulate post-transcriptional gene expressions by binding to the 3' untranslated region (UTR) of target genes [8]. Previous studies have shown that microRNAs are involved in modulating ROS production and cardiomyocyte survival and have critical roles in mediating doxorubicin-induced cardiac dysfunction. Zhao et al. recently showed that miR-140-5p directly targeted NRF2 and SIRT2 to promote oxidative damage and cardiac dysfunction in doxorubicin-induced myocardial toxicity, but inhibition of miR-140-5p prevented against oxidative stress and cardiac impairment in doxorubicin-treated mice [9,10]. Also, miR-375 was shown to act as a tumor-suppressing microRNA that inhibited tumor growth, while knockdown of miR-375 promoted invasion and metastasis of cancer cells [11]. Nezami et al. showed that miR-375 was involved in mediating palmitate-induced enteric neuronal cell apoptosis,

and that systemic injection of miR-375 inhibitor increased the survival of enteric neurons and gastrointestinal motility [12]. Also, miR-375 has roles in the pathogenesis of cardiovascular disease, with increased expression in human and murine failing hearts [13]. Direct inhibition of myocardial miR-375 reduced the inflammatory response and enhanced cardiomyocyte survival in ischemic hearts [13]. Recently, Feng et al. showed that in a rat model of hypertension, inhibition of miR-375-3p reduced Ang II-induced hypertrophy of rat cardiomyocytes by promoting the expression of lactate dehydrogenase B (LDHB) [14].

However, the potential role of miR-375 in doxorubicin-induced oxidative stress and cardiomyocyte apoptosis remains unclear. Therefore, this study aimed to investigate the effects and mechanisms of inhibition of miR-375 in a mouse model of doxorubicin-induced cardiac toxicity *in vivo* and in doxorubicin-treated rat and mouse cardiomyocytes *in vitro*.

Material and Methods

Reagents and antibodies

Doxorubicin was obtained from Sigma-Aldrich (St. Louis MO, USA). The locked nucleic acid (LNA) modified miR-375 inhibitor was purchased from Exiqon A/S (Skelstedet, Vedbaek, Denmark). The scrambled oligo control (CTRL) was obtained from Applied Biosystems (Foster City, CA, USA). The 3-nitrotyrosine (3-NT) and 4-hydroxynonenal (4-HNE) enzyme-linked immunosorbent assay (ELISA) kits were purchased from Abcam (Cambridge, MA, USA). Malondialdehyde (MDA), glutathione (GSH), oxidized glutathione (GSSG), lactic dehydrogenase (LDH), superoxide dismutase (SOD), catalase (CAT), and NADPH oxidase (NOX) assay kits were obtained from Jiancheng Bioengineering Institute (Nanjing, China). The TUNEL detection kit was purchased from Millipore (Billerica, MA, USA). The cell counting kit-8 (CCK-8) assay kit was purchased from Beyotime (Shanghai, China). Antibodies to phosphorylated protein kinase B and AKT (p-PKB/AKT, #13038), total AKT (t-AKT, #4691), and GAPDH (#5174) were obtained from Cell Signaling Technology (Danvers, MA, USA). The antibody to 3-phosphoinositide-dependent protein kinase 1 (PDK1, #ab110025) was obtained from Abcam (Cambridge, UK). MK2206, an inhibitor of AKT, was purchased from MedChemExpress (Shanghai, China). Small interfering RNA against PDK1 (siPDK1) and the scrambled control RNA (siRNA) were both generated by RiboBio Co. Ltd. (Guangzhou, China).

Study design and development of the mouse model of doxorubicin-induced cardiac toxicity

All animal experiments were performed in accordance with the guidelines of the Animal Ethics Committee of Tianjin Medical

University General Hospital, and with the Guide for the Care and Use of Laboratory Animals published by the National Institutes of Health (NIH). Male C57BL/6 mice were housed in a temperature-controlled room with free access to water and food, and were acclimated for at least one week before the study commenced. Mice were intraperitoneally injected with doxorubicin (15 mg/kg diluted in 0.9% saline) for eight days to generate the mouse model of doxorubicin-induced myocardial toxicity, and mice assigned to the control groups were treated with an equal volume of normal saline [2]. Immediately after doxorubicin injection, the mice received a single subcutaneous injection of the locked nucleic acid (LNA) modified miR-375 inhibitor (10 mg/kg) or control (CTRL), as previously described [13]. Three days before doxorubicin injection, the mice were pretreated with the AKT inhibitor, MK2206, by intraperitoneal injection at a dose of 66 mg/kg on alternate days, investigate the role of AKT in the effects of miR-375 [15]. Also, mice were injected intraperitoneally three times with doxorubicin (5 mg/kg) once a week, with a total cumulative dose of 15 mg/kg, to generate the model of doxorubicin-induced myocardial toxicity, as previously described [2].

Assessment of cardiac function in the mouse model

Echocardiography and cardiac catheterization were performed to assess cardiac function in the mouse model, as previously described [16,17]. Mice were anesthetized with 2% isoflurane using an isoflurane delivery system (Viking Medical, Medford, NJ, USA) with the mice placed in a supine position on a warming pad. Echocardiographic parameters were captured by the Vevo 770 ultrasound system (Visual Sonics, Toronto, Canada) equipped with a 30 MHz linear transducer. The images were analyzed using EchoPAC PC SW 3.1.3 software (GE Healthcare Life Sciences, Logan, UT, USA). All imaging and analysis were performed by a sonographer who was unaware of the study groups. Hemodynamic parameters were detected using a 1F microtip pressure-volume catheter (PVR 1045) (Millar Instruments, Houston, TX, USA) that was linked to a PowerLab/4SP image acquisition system (ADInstruments Inc., Sydney, Australia), as previously described [18,19].

Isolation of adult murine cardiomyocytes (AMCs) and determination of the contractile capacity

AMCs were separated through a temperature-controlled Langendorff system to investigate the contractile capacity of cardiomyocytes *in vitro* [20]. Cell contractile capacity was evaluated using the SoftEdge Myocam system (IonOptix Corporation, Milton, MA, USA), as previously described [21]. AMCs were monitored using an Olympus IX53 inverted microscope (Olympus, Tokyo, Japan). The cells were washed with HEPES buffer and stimulated with a high threshold voltage at a frequency of 0.5 Hz. Cell contraction (or shortening) and cell relaxation (or lengthening) parameters measured included the resting length, peak shortening,

the maximal velocity of shortening and lengthening ($\pm$dL/dt), time to peak shortening (TPS), and time to 90% re-lengthening (TR90) were analyzed using the SoftEdge Myocam system (IonOptix Corporation, Milton, MA, USA). AMCs from each group were incubated with fura-2-acetoxymethyl ester (Fura-2AM) (0.5 µM) for 15 minutes, and the fluorescence levels were recorded with a dual-excitation fluorescence photomultiplier system (IonOptix Corporation, Milton, MA, USA), according to the method previously described [21]. Resting fura-2AM fluorescence intensity (FFI), the change in FFI (ΔFFI), and the fluorescence decay time (single exponential and bi-exponential) were calculated for the analysis of transient intracellular Ca^{2+} [22]. Sarcoplasmic reticulum enriched microsomal samples were prepared to detect Ca^{2+}-ATPase (SERCA2α) activity, as previously described [23]. The difference in ATPase activity in sarcoplasmic reticulum enriched microsomes with or without the SERCA inhibitor, thapsigargin, was calculated by measuring SERCA2α activity.

Culture and treatment of H9c2 cells

H9c2 rat cardiac myocytes were purchased from American Type Culture Collection (ATCC) (Manassas, VA, USA), and were cultured in Dulbecco's modified Eagle's medium (DMEM) containing 10% fetal bovine serum (FBS) for 24 hours to achieve confluence. The H9c2 cells were pretreated with miR-375 inhibitor (50 nM) or the control using Lipofectamine RNAiMAX (Invitrogen, Carlsbad, CA, USA) for 24 hours, followed by incubation with doxorubicin (1 µM) for an additional 24 hours. The cells were pre-incubated with the AKT inhibitor, MK2206 (1 µM), for 24 hours. H9c2 cells were transfected with siPDK1 (50 nM) to knockdown PDK1 expression, or siRNA as the negative control, as previously described [26,27]. The mean results of the data from studies performed in triplicate were analyzed by investigators who were unaware of the assignment of the study groups.

Western blot

Total proteins were isolated from myocardial tissues or cultured cells and were then separated using sodium dodecyl sulfate-polyacrylamide gel electrophoresis (SDS-PAGE) [28]. Proteins were transferred to polyvinylidene fluoride (PVDF) membranes, which were then identified with the indicating antibodies overnight at 4°C after blocking with 5% dried skimmed milk powder. After incubating the membranes with the secondary antibodies at room temperature for 1 hour, the membranes were scanned, and the bands were quantified with the ChemiDoc™ Touch Imaging System (Bio-Rad, USA), as previously described [29].

Quantitative real-time polymerase chain reaction (qRT-PCR)

Total RNA was extracted from the left ventricles of the mouse model or from cultured H9c2 cells using TRIzol reagent

(Invitrogen, Carlsbad, CA, USA), as previously described [30,31]. Levels of miR-375, BAX, and BCL-2 were quantified by qRT-PCR using a C1000 Touch Thermal Cycler CFX96™ Real-Time System and iQ™ SYBR Green Supermix (Bio-Rad, Hercules, CA, USA), according to the manufacturer's instructions.

Biochemical analysis

N-terminal pro-brain natriuretic peptide (NT-proBNP), creatine kinase (CK), and cardiac troponin T (cTnT) were detected using a Beckman Coulter Access 2 Immunoassay System analyzer (Beckman Coulter, Brea, CA, USA). Also, 3-NT, MDA, 4-HNE, the ratio between GSH and GSSG (GSH/GSSG), LDH, SOD, CAT, and NOX enzyme activities were quantified using the enzyme-linked immunosorbent assay (ELISA), as previously described [26]. Protein carbonyls were measured by spectrophotometry at 360 nm, as previously described [32].

TUNEL staining, cell viability, and measurement of caspase-3 activity

TUNEL staining was performed to detect cell apoptosis in the myocardium, as previously described [33]. The apoptotic index in the mouse myocardium was calculated as the percentage of TUNEL-positive cell nuclei and the total nuclei. Caspase-3 activity was detected using a commercial colorimetric assay kit (R&D Systems, Minneapolis, MN, USA) [34]. Cell lysates were centrifuged, and the supernatant was collected for the assessment of caspase-3 activity using the colorimetry peptide substrate for caspase-3, Ac-DEVD-pNA. The cell counting kit-8 (CCK-8) assay was used to determine cell viability, as previously described [35,36].

Dual-luciferase reporter assay

Plasmids carrying the wild type (WT) or mutant (MUT) 3' UTR of the PDK1 gene were prepared by RiboBio. Co., Ltd. (Guangzhou, China) and were inserted into the psi-CHECK2™ luciferase reporter plasmid (Promega, Madison, WI, USA). The WT or MUT reporter plasmids were co-transfected with the miR-375 mimic (50 nM) or the negative control, and the luciferase intensity was assessed by the double-luciferase reporter assay kit (Promega, Madison, WI, USA) using the Dual-Light Chemiluminescent Reporter Gene Assay System (Berthold Technologies, Bad Wildbad, Germany) [37].

Statistical analysis

Experimental data were expressed as the mean±standard deviation (SD). Statistical analysis was performed with SPSS version 23.0 software (IBM Corp., Armonk, NY, USA). Comparisons between two groups were performed using the unpaired Student's t-test. Multiple groups were compared using one-way analysis of variance (ANOVA) followed by Tukey's post hoc test. The Mantel-Cox log-rank test was performed to compare the survival data. A P-value <0.05 was considered to be statistically significant.
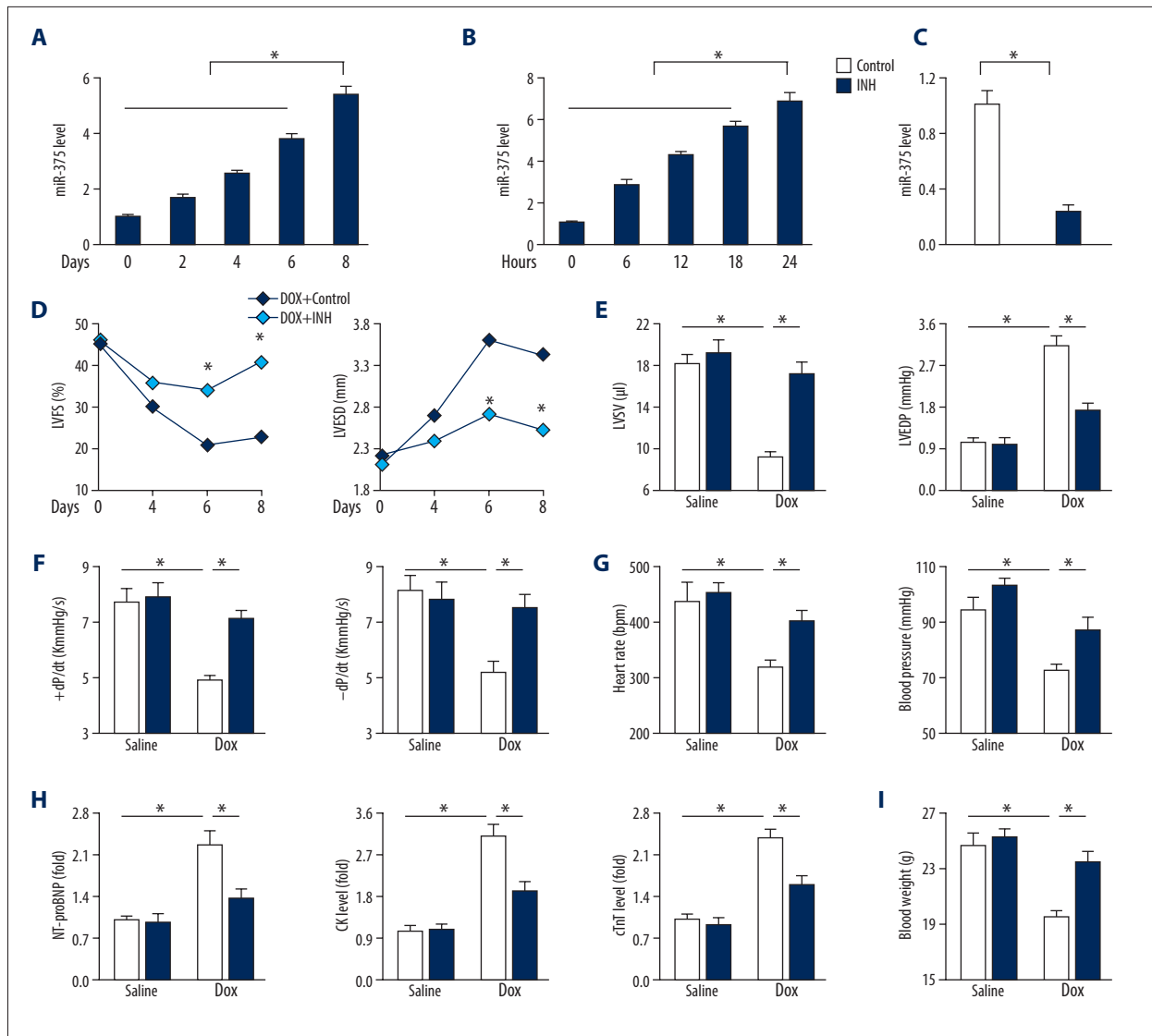
Results

Inhibition of microRNA-375 (miR-375) reduced doxorubicin-induced myocardial toxicity in the mouse model *in vivo*

Figure 1A and 1B show that doxorubicin treatment significantly increased miR-375 expression in murine hearts and H9c2 cardiomyocytes, indicating a role of miR-375 in the pathogenesis of doxorubicin-induced myocardial toxicity. The locked nucleic acid (LNA) modified miR-375 inhibitor was used to suppress miR-375 expression, or the scrambled oligo control (CTRL) was used (Figure 1C). Functional parameter measurements in the mouse model showed that doxorubicin administration caused systolic dysfunction, which was reduced by miR-375 inhibition, as shown by an increased left ventricular fractional shortening (LVFS) and a reduced left ventricular end-systolic dimension (LVESD) (Figure 1D). Mice in the model that were treated with doxorubicin had reduced left ventricular stroke volume (LVSV), the maximal velocity of shortening and lengthening (±dL/dt), and increased left ventricular end-diastolic pressure (LVEDP). These changes were reduced in mice with miR-375 inhibition (Figures 1E, 1F). Also, the heart rate and blood pressure were reduced (Figure 1G).

Consistent with the changes in cardiac function in the mouse model, doxorubicin-treated mice showed increased serum levels of N-terminal pro-brain natriuretic peptide (NT-proBNP), creatine kinase (CK), and cardiac troponin T (cTnT), which were all suppressed in mice treated with the miR-375 inhibitor (Figure 1H). Doxorubicin treatment resulted in whole body cachexia, or reduced body weight, while inhibition of miR-375 significantly preserved the body weight in mice after injection with doxorubicin (Figure 1I). These findings showed that inhibition of miR-375 reduced doxorubicin-induced myocardial toxicity *in vivo* in the mouse model.

Inhibition of miR-375 reduced contractile dysfunction of doxorubicin-treated adult murine cardiomyocytes (AMCs) *in vitro*

As shown in Figure 2A, inhibition of miR-375 prevented the increase in resting length and the decrease in peak shortening of adult murine cardiomyocytes (AMCs) after doxorubicin treatment. AMCs that were isolated from doxorubicin-treated murine hearts also showed a significant change in the maximal velocity of shortening and lengthening (±dL/dt), which
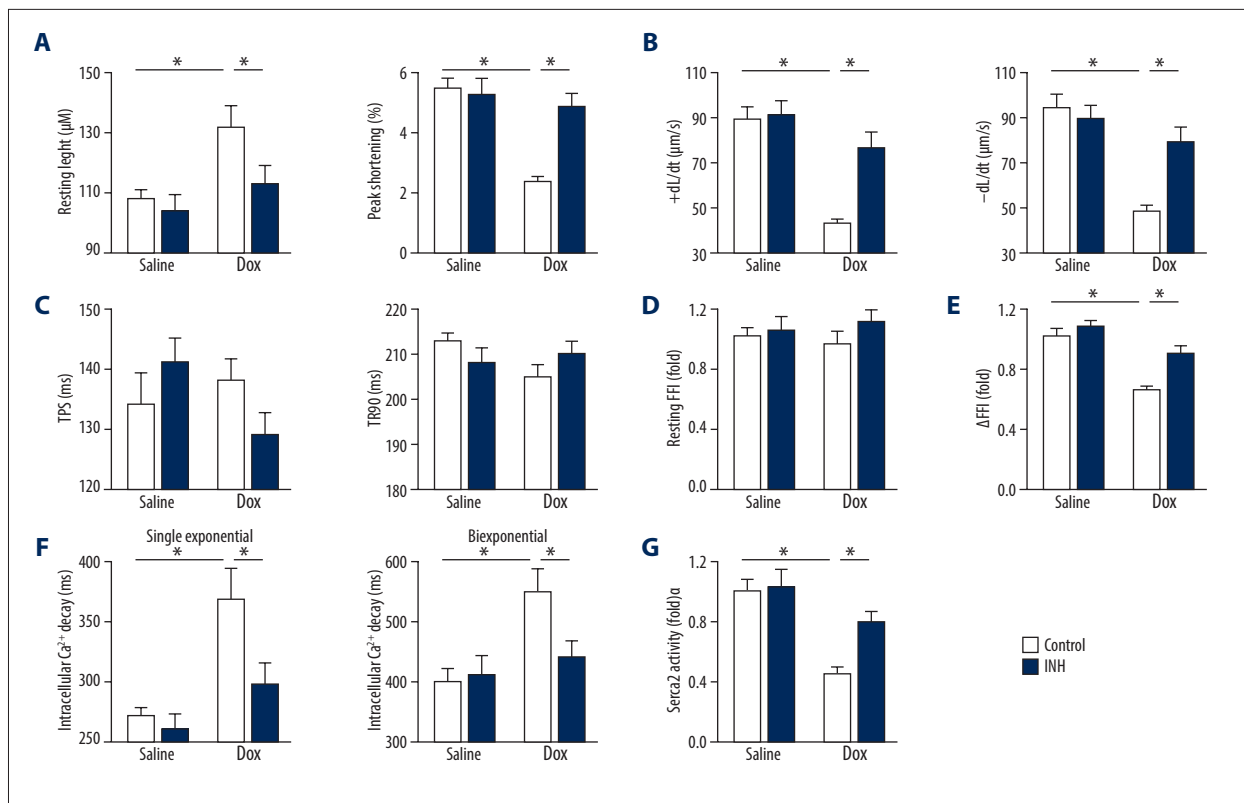
Figure 1. Inhibition of microRNA-375 (miR-375) reduced doxorubicin-induced myocardial toxicity *in vivo*. (**A**) Relative miR-375 level in the myocardium after doxorubicin treatment (n=6). (**B**) Relative miR-375 expression in cultured H9c2 cells after doxorubicin incubation (n=6). (**C**) The efficiency of miR-375 inhibitor in murine hearts (n=6). (**D**) Statistical results of left ventricular fractional shortening (LVFS) and left ventricular end-systolic dimension (LVESD) in indicating time points (n=8). (**E**) Statistical results of left ventricular stroke volume (LVSV) and left ventricular end-diastolic pressure (LVEDP) in mice treated with miR-375 inhibitor (INH) or the negative control (CTRL) after doxorubicin injection (n=8). (**F**) Quantitative results of the maximal velocity of shortening and re-lengthening (±dL/dt) (n=8). (**G**) Heart rate and blood pressure parameters (n=8). (**H**) Serum concentrations of N-terminal pro-brain natriuretic peptide (NT-proBNP), creatine kinase (CK) and cardiac troponin T (cTnT) (n=6). (**I**) Mouse body weight changes (n=8). All data are presented as the mean ± standard deviation (SD). * P<0.05 when compared with the matched group.

was partially reduced in the presence of the miR-375 inhibitor (Figure 2B). However, neither doxorubicin nor miR-375 inhibition significantly changed the time to peak shortening (TPS) and the time to 90% re-lengthening (TR90) (Figure 2C).

Ca^{2+} plays critical roles in regulating cardiomyocyte contractility, and the intracellular Ca^{2+} properties were studied in isolated AMCs. As shown in Figure 2D, there was no significant difference in resting fura-2AM fluorescence intensity (FFI) following the inhibition of miR-375. However, the change in FFI (ΔFFI) was significantly changed in AMCs isolated from doxorubicin-treated hearts, and doxorubicin-induced increase of intracellular Ca^{2+} decay (single- and biexponential curve fit) was equally improved by inhibition of miR-375 (Figure 2E, 2F). Also, inhibition of miR-375 partially restored doxorubicin-induced suppression of SERCA2α activity (Figure 2G). These findings

Figure 2. Inhibition of microRNA-375 (miR-375) reduced contractile dysfunction of doxorubicin-treated adult murine cardiomyocytes (AMCs) *in vitro*. (**A**) The resting length and peak shortening of adult murine cardiomyocytes (AMCs) (n=6). (**B**) The maximal velocity of shortening and re-lengthening (±dL/dt) (n=6). (**C**) Time to peak shortening (TPS) and time to 90% re-lengthening (TR90) in AMCs that analyzed by the IonOptix SoftEdge software (n=6). (**D**) Resting fura-2-acetoxymethyl ester (Fura-2AM) fluorescence intensity (FFI) in AMCs (n=6). (**E**) The alteration of FFI (ΔFFI) in AMCs (n=6). (**F**) Intracellular Ca^{2+} decay rate (single exponential and biexponential) in AMCs (n=8). (**G**) Ca^{2+}-ATPase (SERCA2α) activity in AMCs (n=6). All data are presented as the mean±standard deviation (SD). * P<0.05 when compared with the matched group.

showed that inhibition of miR-375 reduced contractile dysfunction in doxorubicin-treated cardiomyocytes studied *in vitro*.
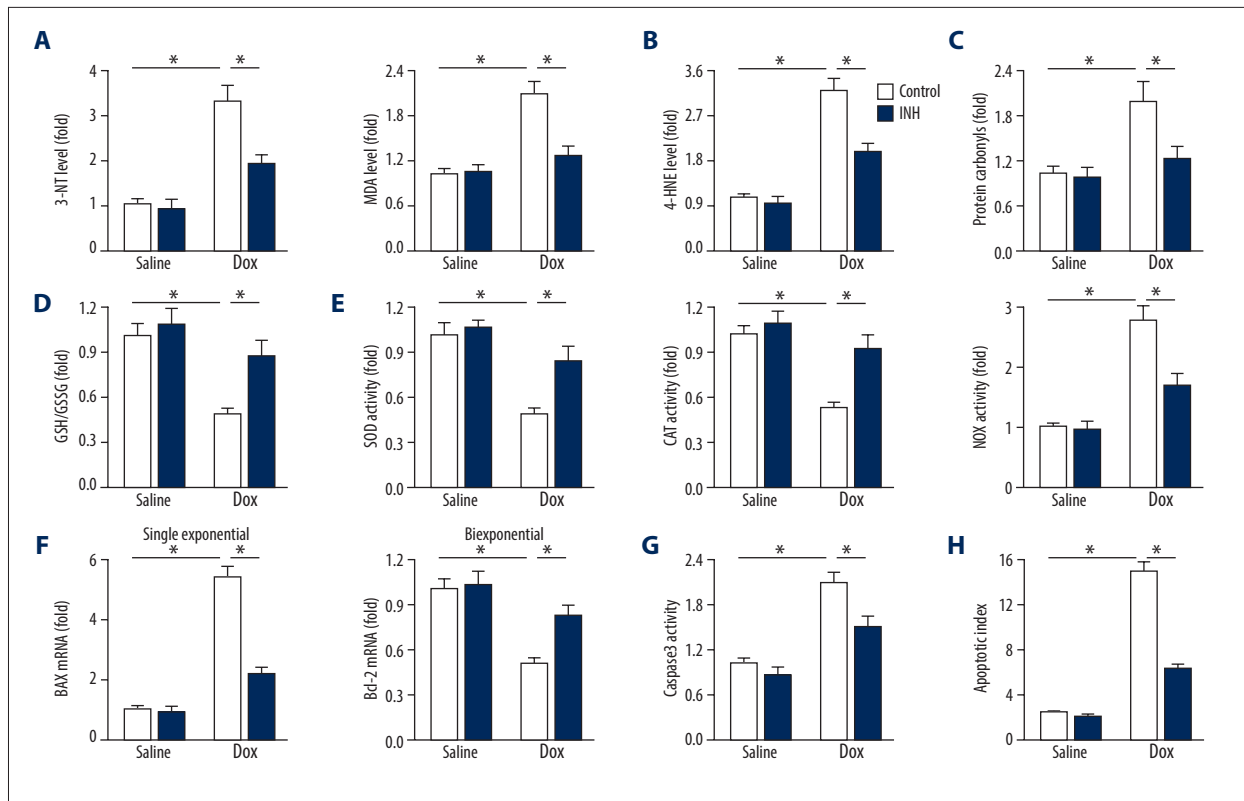
Inhibition of miR-375 reduced oxidative damage in the mouse model of doxorubicin-induced cardiac toxicity

Oxidative stress is involved in the initiation and progression of doxorubicin-induced cardiac dysfunction [2]. As shown in Figure 3A–3D, in the mouse model, doxorubicin injection triggered enhanced oxidative stress within the myocardium, as shown by the increased levels of 3-nitrotyrosine (3-NT), malondialdehyde (MDA), 4-hydroxynonenal (4-HNE), glutathione (GSH), oxidized glutathione (GSSG), and protein carbonyls, which were significantly suppressed by miR-375 inhibition. Also, the miR-375 inhibitor reduced the inhibitory activities of superoxide dismutase (SOD) and catalase (CAT), and increased the activity of NADPH oxidase (NOX) in doxorubicin-treated murine hearts (Figure 3E).

Oxidative stress has previously been shown to be associated with cardiomyocyte apoptosis in doxorubicin-treated cardiac impairment [7]. In this study, the mRNA level of BAX, which encodes a pro-apoptotic molecule, was upregulated, whereas the mRNA level of BCL-2, which encodes an anti-apoptotic molecule, was down-regulated in doxorubicin-treated murine hearts, which were both reversed by the miR-375 inhibitor (Figure 3F). Caspase-3 activity and the TUNEL assay results supported that inhibition of miR-375 significantly prevented cardiomyocyte apoptosis caused by doxorubicin (Figures 3G, 3H). Therefore, in the mouse model of doxorubicin-induce cardiotoxicity, inhibition of miR-375 reduced oxidative damage *in vivo*.

Inhibition of miR-375 protected cardiomyocytes from doxorubicin-induced oxidative damage *in vitro*

Consistent with the *in vivo* data, inhibition of miR-375 significantly reduced the upregulation of 3-NT and MDA in doxorubicin-treated H9c2 cardiomyocytes (Figure 4A). Doxorubicin-induced down-regulation of SOD activity and upregulation of

Figure 3. Inhibition of microRNA-375 (miR-375) reduced cardiac oxidative damage in doxorubicin-treated mice *in vivo*. (**A**) Myocardial 3-nitrotyrosine (3-NT) and 4-hydroxynonenal (4-HNE) levels in mice (n=6). (**B**) Myocardial 4-HNE content (n=6). (**C**) Quantified data of protein carbonyls in mouse hearts (n=6). (**D**) Glutathione (GSH) to oxidized glutathione (GSSG) ratio (n=6). (**E**) Quantitative data of superoxide dismutase (SOD), catalase (CAT) and NADPH oxidase (NOX) activities (n=6). (**F**) Relative mRNA levels of BAX and BCL-2 in doxorubicin-treated hearts (n=6). (**G**) Data on caspase-3 activity (n=6). (**H**) Quantitative data on the apoptotic index in the myocardium (n=6). All data are presented as the mean±standard deviation (SD). * P<0.05 when compared with the matched group.

NOX activity were both prevented by inhibition of miR-375 (Figure 4B, 4C). Induction of BAX and suppression of BCL-2 expression were also prevented by inhibition of miR-375 in the presence of doxorubicin (Figure 4D). Incubation of H9c2 cells in doxorubicin caused damage to the cardiomyocytes, as shown by the increase in caspase-3 activity and the release of lactate dehydrogenase (LDH), which was reduced by the miR-375 inhibitor (Figures 4E, 4F). Further investigation of cell viability also showed that inhibition of miR-375 protected H9c2 cardiomyocytes from doxorubicin-induced oxidative damage *in vitro* (Figure 4G).

Inhibition of miR-375 had protective effects against oxidative damage, which were removed by the AKT inhibitor *in vivo* and *in vitro*

AKT is a key regulator of cell survival, which has recently been reported to modulate doxorubicin-induced oxidative stress [2]. As shown in Figure 5A, treatment with doxorubicin suppressed AKT activation in H9c2 cells, and inhibition of miR-375 reduced this effect. The role of AKT was investigated by pretreatment of the H9c2 cells with MK2206, an inhibitor of AKT, which abolished miR-375 inhibition-mediated down-regulation of 3-NT and MDA (Figure 5B). Also, the reduced cardiomyocyte apoptosis resulting from miR-375 inhibition was also blocked in cells pretreated with MK2206, as shown by the increased levels of caspase-3 activity, LDH release, and reduced cell viability (Figure 5C–5E).

In support of the *in vitro* findings, AKT phosphorylation was preserved in mouse hearts in the doxorubicin-induced toxicity model following inhibition of miR-375 (Figure 5F). Doxorubicin treatment induced the upregulation of MDA and NOX activity, and the down-regulation of SOD activity, which were all improved following inhibition of miR-375, but not in mice with AKT inhibition (Figure 5G, 5H). The effect of the AKT inhibitor, MK2206, was studied in the doxorubicin-treated murine hearts. Figure 5I and 5J show the protective effect on cell loss by miR-375 suppression, which was reduced in the presence of MK2206. Also, the improved cardiac function and
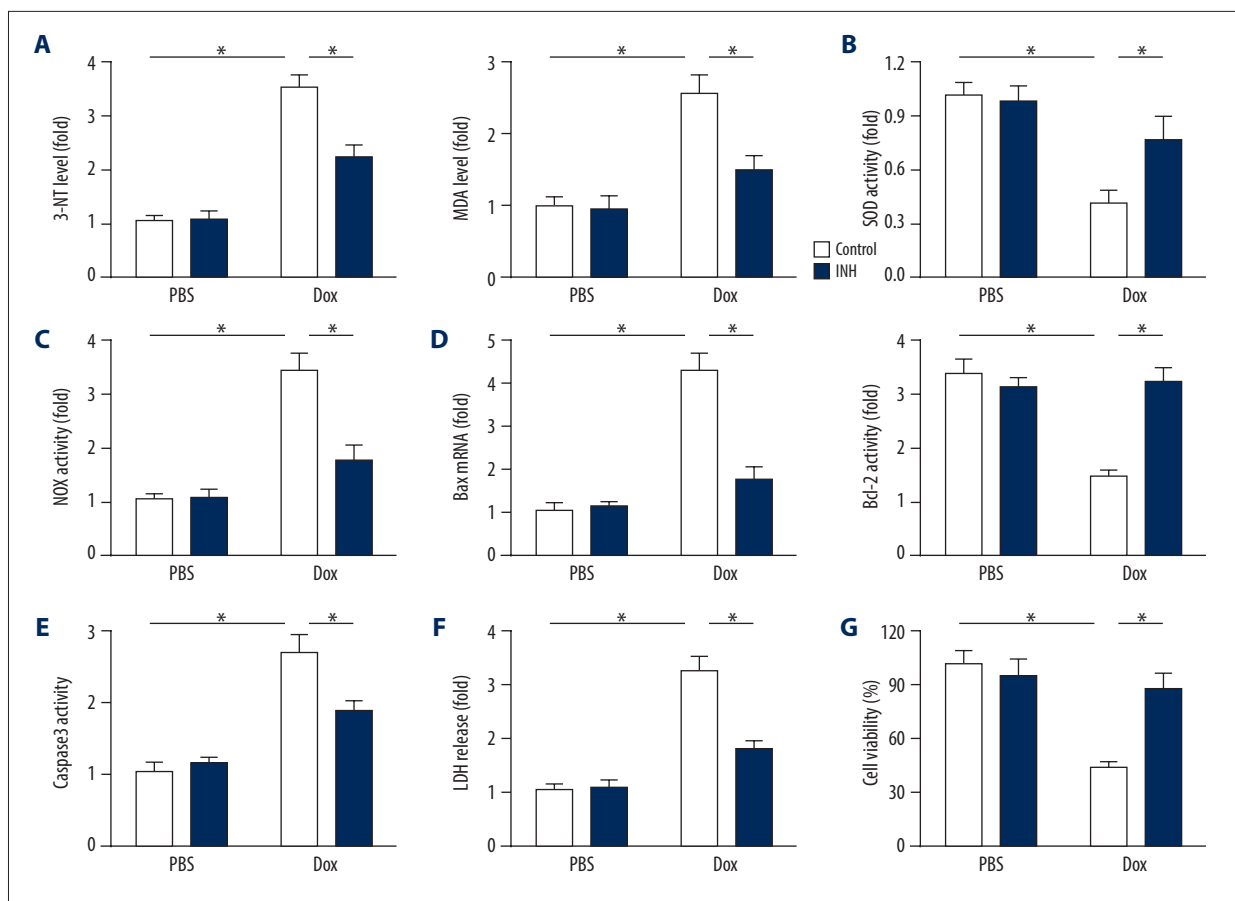
Figure 4. Inhibition of microRNA-375 (miR-375) protected cardiomyocytes from doxorubicin-induced oxidative damage *in vitro*. (**A**) The 3-nitrotyrosine (3-NT) and 4-hydroxynonenal (4-HNE) levels in H9c2 cells after doxorubicin treatment with or without miR-375 inhibitor (n=6). (**B**) Quantitative data of superoxide dismutase (SOD) activity (n=6). (**C**) Quantitative data on NADPH oxidase (NOX) activity in doxorubicin-treated H9c2 cells with or without miR-375 inhibitor (n=6). (**D**) Relative mRNA levels of BAX and BCL-2 after doxorubicin treatment with or without miR-375 inhibition (n=6). (**E**) Quantitative data of caspase-3 activity (n=6). (**F**) Quantitative data on lactate dehydrogenase (LDH) release by H9c2 cells (n=6). (**G**) Cell viability detection (n=8). All data are presented as the mean±standard deviation (SD). * P<0.05 when compared with the matched group.

decreased serum cTnT levels were both reduced by AKT inhibition (Figure 5K ,5L). These findings indicated that the AKT pathway was involved in the miR-375 inhibition-mediated protective effects on oxidative cardiomyocyte damage *in vivo* and *in vitro*.

Inhibition of miR-375 activated the AKT pathway by directly targeting PDK1 in H9c2 cells *in vitro*

Previous studies identified the PDK1 gene as a predicted target of miR-375, which is a gene that encodes a key upstream kinase for the regulation of AKT phosphorylation [12,13]. A putative binding site of miR-375 in the 3' UTR of PDK1 was identified, and the level of PDK1 was assessed after miR-375 inhibition in H9c2 cells (Figure 6A). A shown in Figure 6B, PDK1 was upregulated in cells transfected with miR-375 inhibitor with or without incubation in doxorubicin, indicating that PDK1 was

a potential target of miR-375 in H9c2 cardiomyocytes *in vitro*. To determine whether PDK1 was a direct target of miR-375, the dual-luciferase reporter assay was performed. There was significantly reduced luciferase activity following the treatment of H9c2 cells with the miR-375 inhibitor when compared with the negative control. However, no change in luciferase activity was detected when the miR-375 binding sequence in the 3' UTR of the PDK1 gene was mutated (Figure 6C).

To further evaluate the role of PDK1, its expression was knocked down in H9c2 cardiomyocytes (Figure 6D). PDK1 silencing reduced the activation of AKT in cells following miR-375 inhibition (Figures 6E, 6F). In PDK1-deficient cells, miR-375 inhibition resulted in no protection against doxorubicin-induced oxidative stress, as shown by the sustained production of 3-NT and MDA (Figure 6G, 6H). Reduction in cardiomyocyte apoptosis following miR-375 inhibition was also completely
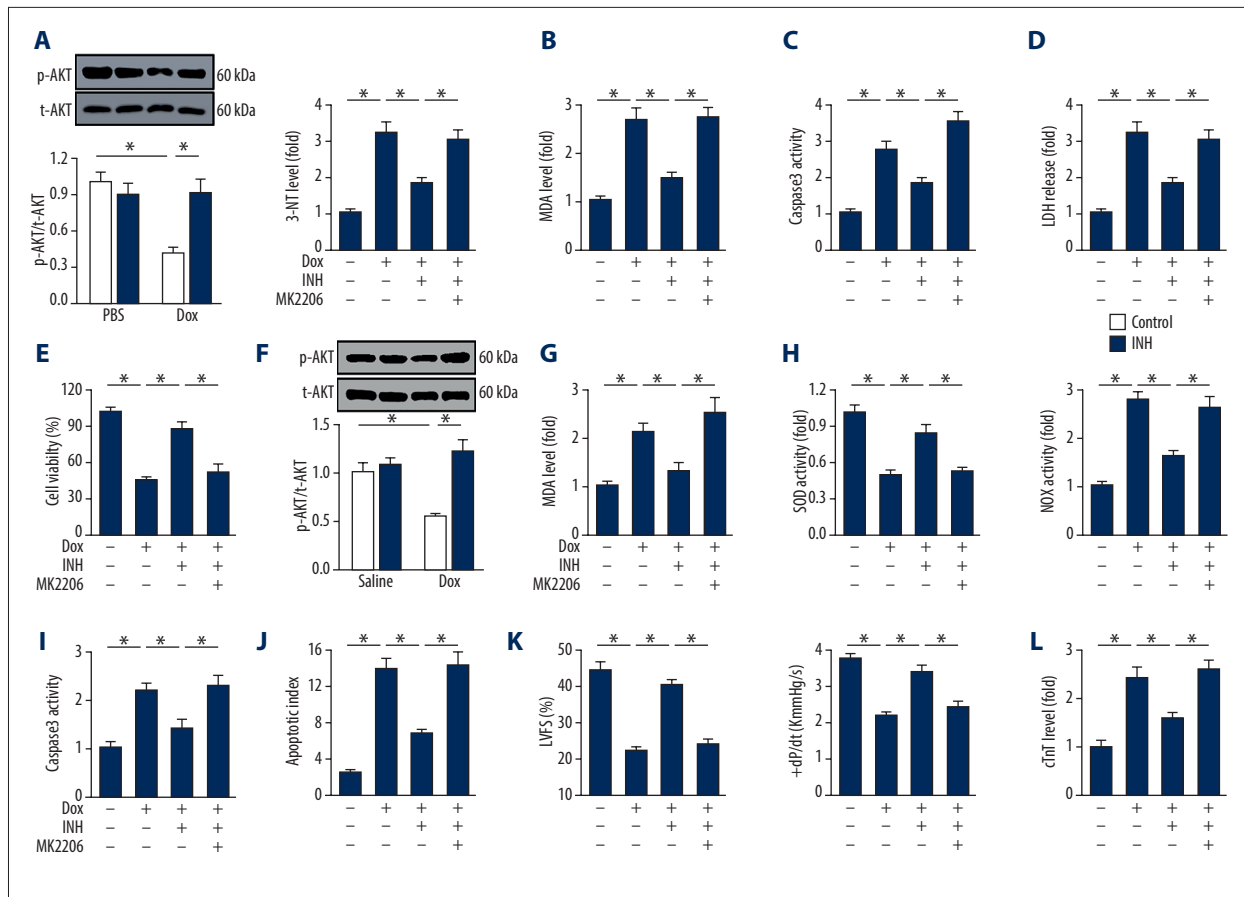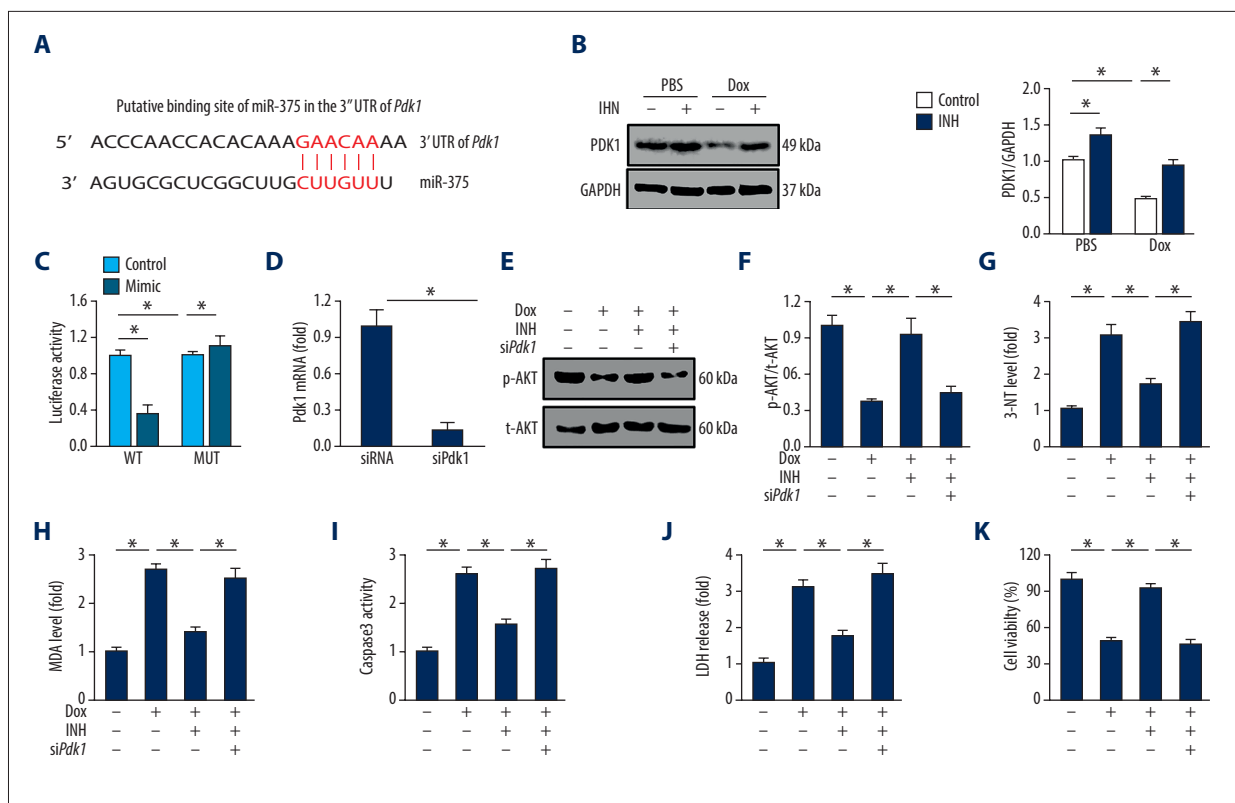
Figure 5. Inhibition of microRNA-375 (miR-375) resulted in protective effects on oxidative damage were removed by AKT inhibitor *in vivo* and *in vitro*. (**A**) Representative images of the Western blot and the quantitative results *in vitro* (n=6). (**B**) The 3-nitrotyrosine (3-NT) and 4-hydroxynonenal (4-HNE) levels in cultured cells after treatment with the AKT inhibitor, MK2206 (n=6). (**C**) Quantitative data of caspase-3 activity in cultured cells with AKT suppression (n=6). (**D**) Statistical results of lactate dehydrogenase (LDH) release by H9c2 cells (n=6). (**E**) Quantification of cell viability by cell counting kit-8 (CCK-8) assay (n=8). (**F**) Representative images of the Western blot data and the corresponding quantification in mice (n=6). (**G**) Myocardial malondialdehyde (MDA) levels in the indicated groups (n=6). (**H**) Superoxide dismutase (SOD) and NADPH oxidase (NOX) activities in mice (n=6). (**I**) Quantitative data of caspase-3 activity in murine hearts (n=6). (**J**) The quantitative results of the apoptotic index in murine hearts (n=6). (**K**) Quantification of left ventricular fractional shortening (LVFS) and the maximal velocity of shortening and re-lengthening (±dL/dt) (n=6). (**L**) Serum level of cardiac troponin T (cTnT) in mice (n=6). All data are presented as the mean±standard deviation (SD). * $P < 0.05$ when compared with the matched group.

abolished by siPDK1, as shown by the caspase-3 activity, LDH levels, and cell viability (Figure 6I–6K). These findings supported that miR-375 inhibition activated the AKT pathway by directly targeting PDK1.

Inhibition of miR-375 prevented doxorubicin-induced cardiac toxicity in the mouse model *in vivo*

In addition to the acute myocardial toxicity, doxorubicin treatment has previously been reported to be associated with the chronic myocardial toxicity in up to 1.7% of patients [38]. In this study, inhibition of miR-375 prevented doxorubicin-induced cardiac toxicity in the mouse model. As shown in Figure 7A and 7B, consecutive injections of low-dose doxorubicin resulted in a

significant decrease in systolic cardiac function, which was improved by miR-375 inhibition. Measurement of the left ventricular stroke volume (LVSV), left ventricular end-diastolic pressure (LVEDP), and ±dP/dt supported that inhibition of miR-375 prevented doxorubicin-induced cardiac impairment *in vivo* in the mouse model (Figure 7C–7E). Myocardial toxicity was also investigated by measuring the serum levels of NT-proBNP and CK, which showed that miR-375 inhibition reduced chronic doxorubicin-induced injury in murine hearts (Figure 7F). Also, doxorubicin-induced mortality of mice in the model group was prevented by miR-375 inhibition (Figure 7G). These findings supported that inhibition of miR-375 could prevent doxorubicin-induced cardiac toxicity in the mouse model.
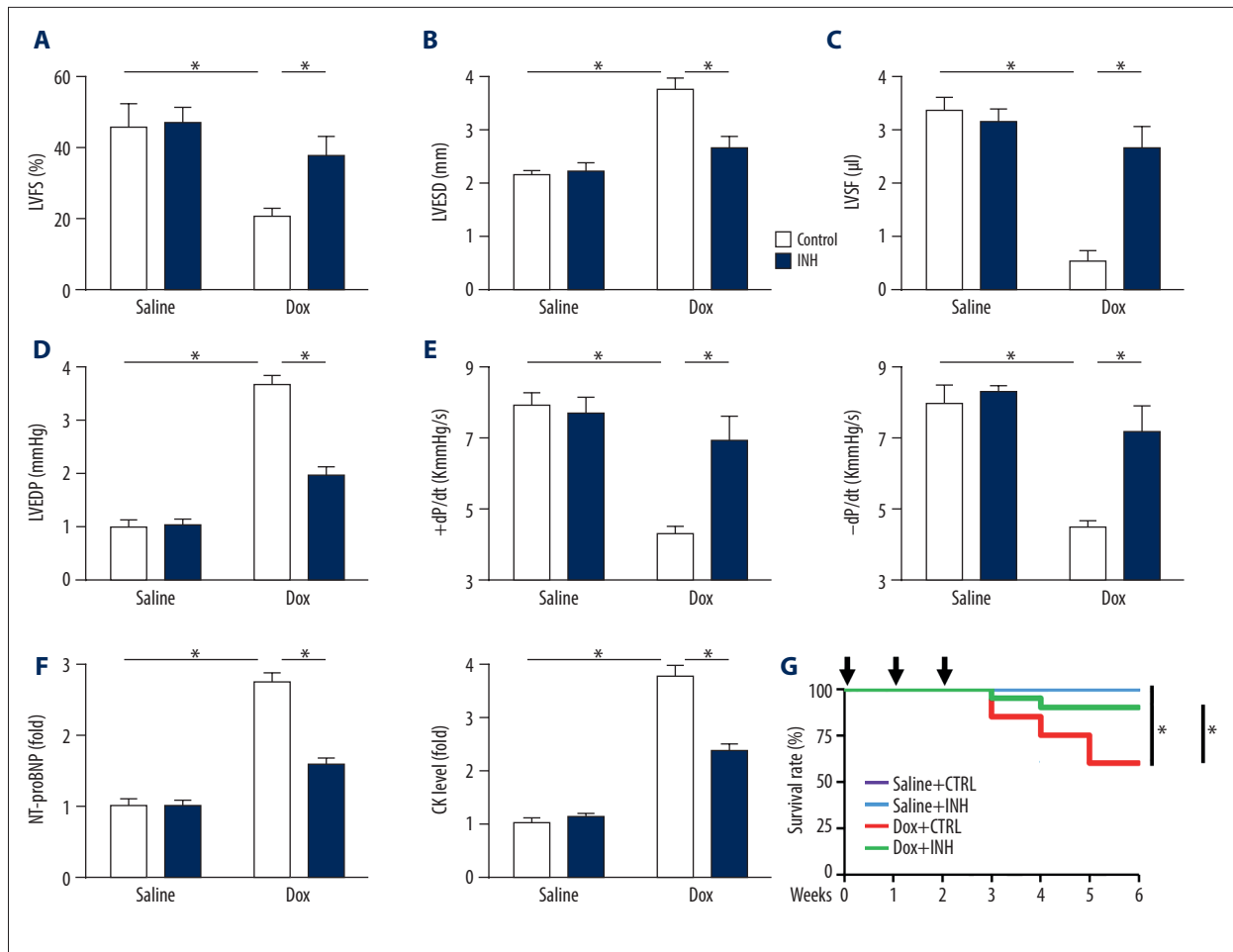
Figure 6. Inhibition of microRNA-375 (miR-375) activated the AKT pathway by directly targeting PDK1. (**A**) The putative binding site of miR-375 in the 3' UTR of the PDK1 gene. (**B**) Representative images of the results of Western blot and the corresponding statistical data (n=6). (**C**) Quantitative data of the luciferase activity with wild type or mutant 3' UTR of the PDK1 gene (n=8). (**D**) The efficiency of siPDK1 *in vitro* (n=6). (**E, F**) Representative images of Western blot and the corresponding statistical data (n=6). (**G, H**) Quantitative data of 3-nitrotyrosine (3-NT) and malondialdehyde (MDA) production by H9c2 cells (n=6). (**I**) Quantitative data on caspase-3 activity (n=6). (**J**) Lactate dehydrogenase (LDH) levels associated with H9c2 cells (n=6). (**K**) Quantification of cell viability using the cell counting kit-8 (CCK-8) assay (n=6). All data are presented as the mean±standard deviation (SD). * P<0.05 when compared with the matched group.

Discussion

This study aimed to investigate the effects of inhibition of microRNA-375 (miR-375) in a mouse model of doxorubicin-induced cardiac toxicity *in vivo* and in doxorubicin-treated rat H9c2 cardiomyocytes and adult murine cardiomyocytes (AMCs) *in vitro*. The findings from this study showed that miR-375 expression was increased by doxorubicin treatment, which then caused PDK1 down-regulation and AKT inactivation, contributing to the development of doxorubicin-induced oxidative damage in murine hearts. However, inhibition of miR-375 significantly reduced doxorubicin-induced myocardial toxicity by activating the PDK1/AKT pathway, and AKT inhibition or PDK1 deficiency removed the protective effects of miR-375 inhibition on doxorubicin-induced oxidative damage. This study also showed that miR-375 inhibition prevented doxorubicin-induced cardiac toxicity. Therefore, it is possible that miR-375 was involved in the regulation of oxidative damage by doxorubicin. These preliminary findings support the need for further studies to

determine the potential role of miR-375 as a therapeutic target for doxorubicin-induced myocardial toxicity.

Multiple factors have been implicated in the initiation and progression of doxorubicin-induced myocardial toxicity. Increased production of reactive oxygen species (ROS) has important and central roles by causing oxidative stress and cell apoptosis within the myocardium [2,10]. Cardiac tissue is particularly vulnerable to damage from free radicals due to the high mitochondrial content and the low levels of antioxidant enzymes. Previous studies have shown that ROS could be detected in hearts within three hours after doxorubicin injection [7]. The findings from the present study showed that doxorubicin treatment further down-regulated superoxide dismutase (SOD) and catalase (CAT) activity and upregulated NADPH oxidase (NOX) activity, resulting in lipid peroxidation, protein carbonyls, and cardiomyocyte apoptosis. Increased ROS generation has previously been shown to disrupt calcium homeostasis, which results in cardiomyocyte contractile dysfunction [39].

Figure 7. Inhibition of microRNA-375 (miR-375) had protective effects on doxorubicin-induced cardiac toxicity in mice *in vivo*. (**A–E**) Statistical results of the left ventricular fractional shortening (LVFS), left ventricular end-systolic dimension (LVESD), left ventricular stroke volume (LVSV), and left ventricular end-diastolic pressure (LVEDP) and the maximal velocity of shortening and re-lengthening (±dL/dt) in mice with consecutive injections of doxorubicin (n=8). (**F**) Serum levels of N-terminal pro-brain natriuretic peptide (NT-proBNP) and creatine kinase (CK) in mice with doxorubicin-induced myocardial toxicity (n=6). (**G**) The survival rate in mice with repeated injections of low-dose doxorubicin (n=20). All data are presented as the mean±standard deviation (SD). * $P<0.05$ when compared with the matched group.

However, inhibition of miR-375 significantly reduced oxidative damage in the mouse model of doxorubicin-induced myocardial toxicity, preventing cardiomyocyte contractile dysfunction and cardiac impairment caused by doxorubicin treatment.

Previous studies have shown that miR-375 has an important role in maintaining normal glucose and in cell survival [12,13]. The findings from the present study supported the findings from previous studies, as the inhibition of miR-375 resulted in the activation of the AKT pathway in a PDK1-dependent manner, and significantly reduced doxorubicin-induced cardiomyocyte apoptosis. Garikipati et al. recently showed that the inhibition of miR-375 reduced cardiomyocyte apoptosis in the ischemic myocardium by restoring the PDK1/AKT axis [13]. Previous studies have also shown that doxorubicin-induced myocardial

toxicity was associated with the decreased AKT phosphorylation, and AKT reactivation by either pharmacological methods or genetic manipulation promoted cardiomyocyte survival and prevented doxorubicin-induced cardiac dysfunction [2]. In addition to its role in regulating cell survival, AKT is also involved in preventing oxidative stress. Zhang et al. recently showed that activation of AKT could reduce doxorubicin-induced oxidative damage by reducing GSK3β/FYN-mediated NRF2 nuclear export and degradation [2]. In the present study, the inhibition of miR-375 resulted in beneficial effects that reduced oxidative damage, which were completely abolished following the use of an AKT inhibitor.

Conclusions

This study aimed to investigate the effects and mechanisms of inhibition of miR-375 in a mouse model of doxorubicin-induced cardiac toxicity *in vivo* and in doxorubicin-treated rat and mouse cardiomyocytes *in vitro*. Inhibition of miR-375 prevented oxidative damage in a mouse model of doxorubicin-induced cardiac toxicity *in vivo* and in doxorubicin-treated rat and mouse cardiomyocytes *in vitro* through the PDK1/AKT signaling pathway.

Conflict of interest

None.

References:

1. Silber JH, Barber G: Doxorubicin-induced myocardial toxicity. N Engl J Med, 1995; 333: 1359–60

2. Zhang X, Hu C, Kong CY et al: FNDC5 alleviates oxidative stress and cardiomyocyte apoptosis in doxorubicin-induced myocardial toxicity via activating AKT. Cell Death and Differentiation, 2019; s41418-019-0372-z

3. Goormaghtigh E, Chatelain P, Caspers J, Ruysschaert JM: Evidence of a complex between adriamycin derivatives and cardiolipin: possible role in myocardial toxicity. Biochem Pharmacol, 1980; 29: 3003–10

4. Kotamraju S, Chitambar CR, Kalivendi SV et al: Transferrin receptor-dependent iron uptake is responsible for doxorubicin-mediated apoptosis in endothelial cells: Role of oxidant-induced iron signaling in apoptosis. J Biol Chem, 2002; 277: 17179–87

5. Vasquez-Vivar J, Martasek P, Hogg N et al: Endothelial nitric oxide synthase-dependent superoxide generation from adriamycin. Biochemistry, 1997; 36(38): 11293–97

6. Myers CE, McGuire WP, Liss RH et al: Adriamycin: The role of lipid peroxidation in cardiac toxicity and tumor response. Science, 1977; 197: 165–67

7. Chaiswing L, Cole MP, St Clair DK et al: Oxidative damage precedes nitrative damage in adriamycin-induced cardiac mitochondrial injury. Toxicol Pathol, 2004; 32: 536–47

8. Gabisonia K, Prosdocimo G, Aquaro GD et al: MicroRNA therapy stimulates uncontrolled cardiac repair after myocardial infarction in pigs. Nature, 2019; 569: 418–22

9. Zhao L, Tao X, Qi Y et al: Protective effect of dioscin against doxorubicin-induced myocardial toxicity via adjusting microRNA-140-5p-mediated myocardial oxidative stress. Redox Biol, 2018; 16: 189–98

10. Zhao L, Qi Y, Xu L et al: MicroRNA-140-5p aggravates doxorubicin-induced myocardial toxicity by promoting myocardial oxidative stress via targeting Nrf2 and Sirt2. Redox Biol, 2018; 15: 284–96

11. Kong KL, Kwong DL, Chan TH et al: MicroRNA-375 inhibits tumour growth and metastasis in oesophageal squamous cell carcinoma through repressing insulin-like growth factor 1 receptor. Gut, 2012; 61: 33–42

12. Nezami BG, Mwangi SM, Lee JE et al: MicroRNA 375 mediates palmitate-induced enteric neuronal damage and high-fat diet-induced delayed intestinal transit in mice. Gastroenterology, 2014; 146: 473–83

13. Garikipati V, Verma SK, Jolardarashi D et al: Therapeutic inhibition of miR-375 attenuates post-myocardial infarction inflammatory response and left ventricular dysfunction via PDK-1-AKT signalling axis. Cardiovasc Res, 2017; 113: 938–49

14. Feng H, Wu J, Chen P et al: MicroRNA-375-3p inhibitor suppresses angiotensin II-induced cardiomyocyte hypertrophy by promoting lactate dehydrogenase B expression. J Cell Physiol, 2019; 234: 14198–209

15. Jeong SH, Kim HB, Kim MC et al: Hippo-mediated suppression of IRS2/AKT signaling prevents hepatic steatosis and liver cancer. J Clin Invest, 2018; 128: 1010–25

16. Wang X, Bi X, Zhang G et al: Glucose-regulated protein 78 is essential for cardiac myocyte survival. Cell Death Differ, 2018; 25: 2181–94

17. Zhang X, Ma ZG, Yuan YP et al: Rosmarinic acid attenuates cardiac fibrosis following long-term pressure overload via AMPKalpha/Smad3 signaling. Cell Death Dis, 2018; 9: 102

18. Deshwal S, Forkink M, Hu CH et al: Monoamine oxidase-dependent endoplasmic reticulum-mitochondria dysfunction and mast cell degranulation lead to adverse cardiac remodeling in diabetes. Cell Death Differ, 2018; 25: 1671–85

19. Zhang X, Zhu JX, Ma ZG et al: Rosmarinic acid alleviates cardiomyocyte apoptosis via cardiac fibroblast in doxorubicin-induced myocardial toxicity. Int J Biol Sci, 2019; 15: 556–67

20. Prola A, Pires DSJ, Guilbert A et al: SIRT1 protects the heart from ER stress-induced cell death through eIF2alpha deacetylation. Cell Death Differ, 2017; 24: 343–56

21. Guo R, Hua Y, Ren J et al: Cardiomyocyte-specific disruption of Cathepsin K protects against doxorubicin-induced myocardial toxicity. Cell Death Dis, 2018; 9: 692

22. Tai Y, Li L, Peng X et al: Mitochondrial uncoupler BAM15 inhibits artery constriction and potently activates AMPK in vascular smooth muscle cells. Acta Pharm Sin B, 2018; 8: 909–18

23. Jiao Q, Takeshima H, Ishikawa Y, Minamisawa S: Sarcalumenin plays a critical role in age-related cardiac dysfunction due to decreases in SERCA2a expression and activity. Cell Calcium, 2012; 51: 31–39

24. Fomison-Nurse I, Saw E, Gandhi S et al: Diabetes induces the activation of pro-ageing miR-34a in the heart, but has differential effects on cardiomyocytes and cardiac progenitor cells. Cell Death Differ, 2018; 25: 1336–49

25. Wang X, Ha T, Liu L et al: TLR3 mediates repair and regeneration of damaged neonatal heart through glycolysis dependent YAP1 regulated miR-152 expression. Cell Death Differ, 2018; 25: 966–82

26. Hu C, Zhang X, Wei W et al: Matrine attenuates oxidative stress and cardiomyocyte apoptosis in doxorubicin-induced myocardial toxicity via maintaining AMPKalpha/UCP2 pathway. Acta Pharm Sin B, 2019; 9: 690–701

27. Ganjam GK, Terpolilli NA, Diemert S et al: Cylindromatosis mediates neuronal cell death *in vitro* and *in vivo*. Cell Death Differ, 2018; 25: 1394–407

28. Mughal W, Martens M, Field J et al: Myocardin regulates mitochondrial calcium homeostasis and prevents permeability transition. Cell Death Differ, 2018; 25: 1732–48

29. Wang K, Ding R, Ha Y et al: Hypoxia-stressed cardiomyocytes promote early cardiac differentiation of cardiac stem cells through HIF-1alpha/Jagged1/Notch1 signaling. Acta Pharm Sin B, 2018; 8: 795–804

30. Sarikhani M, Mishra S, Desingu PA et al: SIRT2 regulates oxidative stress-induced cell death through deacetylation of c-Jun NH2-terminal kinase. Cell Death Differ, 2018; 25: 1638–56

31. Li X, Tian Y, Tu MJ et al: Bioengineered miR-27b-3p and miR-328-3p modulate drug metabolism and disposition via the regulation of target ADME gene expression. Acta Pharm Sin B, 2019; 9: 639–47

32. Efentakis P, Varela A, Chavdoula E et al: Levosimendan prevents doxorubicin-induced myocardial toxicity in time- and dose dependent manner: Implications for inotropy. Cardiovasc Res, 2019 [Epub ahead of print]

33. Afonso MB, Rodrigues PM, Simao AL et al: miRNA-21 ablation protects against liver injury and necroptosis in cholestasis. Cell Death Differ, 2018; 25: 857–72

34. Zhang T, Chen Y, Ge Y et al: Inhalation treatment of primary lung cancer using liposomal curcumin dry powder inhalers. Acta Pharm Sin B, 2018; 8: 440–48

35. Luo M, Wu L, Zhang K et al: miR-137 regulates ferroptosis by targeting glutamine transporter SLC1A5 in melanoma. Cell Death Differ, 2018; 25: 1457–72

36. Zhang Q, Xu C, Lin S et al: Synergistic immunoreaction of acupuncture-like dissolving microneedles containing thymopentin at acupoints in immune-suppressed rats. Acta Pharm Sin B, 2018; 8: 449–57

37. Luo M, Wu L, Zhang K et al: miR-137 regulates ferroptosis by targeting glutamine transporter SLC1A5 in melanoma. Cell Death Differ, 2018; 25: 1457–72

38. Von Hoff DD, Layard MW, Basa P et al: Risk factors for doxorubicin-induced congestive heart failure. Ann Intern Med, 1979; 91: 710–17

39. Zhang M, Prosser BL, Bamboye MA et al: Contractile function during angiotensin-II activation: Increased Nox2 activity modulates cardiac calcium handling via phospholamban phosphorylation. J Am Coll Cardiol, 2015; 66: 261–72